ORIGINAL RESEARCH

Identification of prognostic indicator based on hypoxia-related lncRNAs analysis in lung adenocarcinoma

Jiaojiao Zhang[1], Blessed Kondowe[2], Hui Zhang[3], Xinming Xie[4], Qiang Song[5], Bo Guo[6]*, Jin Shang[3]*

1 Department of Pathology, the First Affiliated Hospital of Xi'an Jiaotong University, Xi'an, P.R. China
2 Radiology Department, Mzuzu Central Hospital, Mzuzu, Malawi
3 Department of Medical Imaging, the First Affiliated Hospital of Xi'an Jiaotong University, Xi'an, P.R. China
4 Department of Respiratory and Critical Care Medicine, the First Affiliated Hospital of Xi'an Jiaotong University, Xi'an, P.R. China
5 Department of Cardiovascular Medicine, the First Affiliated Hospital of Xi'an Jiaotong University, Xi'an, P.R. China
6 Institute of Genetics and Developmental Biology, Translational Medicine Institute, School of Basic Medical Sciences, Xi'an Jiaotong University Health Science Center, Xi'an, P.R. China

***Corresponding Author:Bo Guo and Jin Shang contributed equally to this work**; E-mail: bo_guo@xjtu.edu.cn; shangjin01@qq.com

Abstract

Introduction

There were no systematic studies about hypoxia-related long noncoding RNAs (lncRNAs) signatures to predict the survival of patients with lung adenocarcinoma (LUAD). Setting up matching hypoxia-related lncRNA signatures was necessary.

Objective

This study aimed to establish hypoxia-related lncRNAs signatures and to seek new biomarkers to predict the prognosis of the patients with lung adenocarcinoma.

Methodology

The Cancer Genome Atlas (TCGA) database provided the expression profiles of lncRNAs that includes 535 lung adenocarcinoma samples. The coexpression network of lncRNAs and hypoxia-related different expression genes (DEGs) was utilized to select hypoxia-related lncRNAs. The lncRNAs were further screened using univariate Cox regression. In addition, Lasso regression and multivariate Cox regression were used to develop a hypoxia-related lncRNAs signature. A risk score based on the signature was established, and Cox regression was used to test if it was an independent prognostic factor.

Results

Nine prognostic hypoxia-related lncRNAs (LINC01150, AC010980.2, AL606489.1, AL034397.3, LINC00460, LINC02081, FAM83A-AS1, AL365181.2, and AC026355.1) were identified to be significantly different, which made up a hypoxia-related lncRNAs signature. The high-risk group had shorter OS compared with the low-risk group (P = 3.329e − 09, log-rank test). A risk score based on the signature was a significantly independent factor for the patients with LUAD (HR = 1.449, 95% CI = 1.312 − 1.602, P < 0.001).

Conclusion

The nine hypoxia-related lncRNAs and their signature might be molecular biomarkers and therapeutic targets for the patients with LUAD.

Key words: Hypoxia-related long noncoding RNAs; prognostic; lung adenocarcinoma

Introduction

Lung cancer is the second most common cause of death (> 1.3 million people world-wide every year)[1,2]. In China, lung cancer incidence in both men and women has increased rapidly in recent years, imposing a great threat to human health[3]. Non-small cell lung cancer (NSCLC) accounts for approximately 85% of all lung cancers, and lung adenocarcinoma (LUAD) and squamous cell carcinoma (LUSC) are two major histologic subtypes of NSCLC[4-6]. LUAD is the most common type of NSCLC, which shows distinct genetic drivers and divergent prognostic profiles versus other types of lung cancer[7-9]. Therefore, further research on the pathogenesis, development and prognosis of LUAD will help to discover new targets and therapeutic drugs.

Evidence has been found that hypoxia is one of the common characteristics in rapidly growing solid tumors. The early phase of solid tumor growth can be divided into two steps in hypoxia conditions: First, malignant cells form small solid tumors, resulting in tumor hypoxia due to relative lag of vascular growth and rapid proliferation of tumor cells. Second, hypoxia triggers fundamental changes in gene expression, leading to neovascularization and tumor growth and metastasis[10]. A large number of findings revealed that hypoxia had multiple functions in occurrence, maintenance, and development of tumors, including LUAD[11-14]. However, there are no systematic studies about hypoxia-related gene signatures to predict the survival of patients with LUAD.

Long noncoding RNAs (lncRNAs) are a group of noncoding RNAs with more than 200 bp in length with no or limited protein-coding function, which were first discovered in mice in 2002 and lack of specific and complete open reading frame[15]. Recently, several studies reported that lncRNAs represent some of the most differentially expressed transcripts between lung tumor and normal lung tissues, highlighting their potential in lung cancer initiation and progression[16,17]. It has been found that lncRNAs are involved in the development, invasion and metastasis, prognosis, and the chemoresistance of lung cancer via

https://dx.doi.org/10.4314/mmj.v36i3.3

modulating hypoxia[13,18]. These studies focused on single or a few lncRNAs for LUAD, while the expression of lncRNAs of The Cancer Genome Atlas (TCGA) datasets was not performed to explore novel biomarkers for forecasting the prognosis of LUAD. Therefore, we aimed to utilize TCGA databases to establish hypoxia-related lncRNAs signatures and seek new biomarkers to predict the prognosis of the patients with lung adenocarcinoma.

Materials and Methods

Datasets and sample extraction

We followed the methods of Weige Zhou, et al[19]. The RNA sequencing (RNA-seq) data of LUAD was acquired from The Cancer Genome Atlas (TCGA) database (https://portal.gdc.cancer.gov/). Patients with a LUAD diagnosis and intact lncRNA data as well as clinical information qualified as inclusion criteria. The exclusion criteria: patients with follow-up time less than 30 days. Finally, 535 patients with LUAD were absorbed. Furthermore, the clinical data for the patients was retrieved from the TCGA database. The LIMMA package for R software was used to examine the difference expression genes (DEGs) between LUAD samples and normal samples[20]. Adjusted P value and |log fold change| (|log FC|) were used to evaluate the significance of DEGs, adjusted $P < 0.05$ and $|\log FC| > 1$ were set as the cutoff criteria. R software was used to analyze the DEGs' heatmap and volcano (version 4.0.4).

Screening of lncRNAs and hypoxia-related genes

The RNAseq dataset was used to obtain the lncRNA profiles, and the log2 transformation was used to standardize the total RNA expression data. The list of genes related to hypoxia was downloaded using Gene Set Enrichment Analysis (GSEA) (http://www.gsea-msigdb.org/gsea/msigdb/index.jsp)[21]. The correlation between lncRNAs and hypoxia-related genes was calculated using Pearson correlation. The square of correlation coefficient $|R^2| > 0.3$ and $P < 0.001$ was considered to be hypoxia-related lncRNAs. Finally, Cytoscape software 3.6.1 was employed to picture co-expression networks[22].

Identification of prognostic hypoxia-related lncRNAs

The prognostic value of hypoxia-related lncRNAs was assessed by univariate Cox regression Hypoxia-related lncRNAs with $P < 0.05$ were included in the absolute minimum shrinkage and selection operator (Lasso) regression in the univariate analysis[23]. Then, in order to establish a risk score, the results of Lasso were included into a multivariate Cox model. We found a risk score based on a linear combination of the hypoxia-related lncRNAs expression levels multiplied with a regression coefficient (β): risk score = $\sum_{i=1}^{n} \beta i *$ expression of lncRNAi). Based on the median risk score, the patients were divided into two groups: high-risk and low-risk. Log-rank test was used to compare the survival differences between those two groups.

Development of prognostic model

An independent prognostic model was generated from Cox regression The nomogram was used to predict patient survival[24]. Index of agreement (C-index), calibration curves, and receiver operating characteristic (ROC) curves were used to examine model accuracy. To confirm whether the risk score was an independent prognostic indicator, demographic data were entered into a multivariate Cox regression.

Statistical analysis

The Kaplan-Meier method was used to generate the survival curves and the log-rank test was used for comparison. Cox regression and Lasso regression were utilized to estimate the prognostic impact of the hypoxia-related lncRNAs signature and clinicopathological data. The statistical analyses were conducted in R language (version 4.0.4). $P \leq 0.05$ were considered statistically significant.

Results

Identification of DEGs in LUAD and construction of a coexpression network

In TCGA-LUAD, 14142 lncRNAs and 19658 mRNAs were found together. Then, in TCGA-LUAD datasets, an additional 3061 DEGs for lncRNAs (Figure 1A and 1B) and 4661 DEGs for mRNAs (Figure 1C and 1D) were discovered. 64 hypoxia-related genes in total, of which 64 genes (38 down-regulated and 26 up-regulated) were expressed in lung cancer, were retrieved from GSEA (Table 1).

Nine mRNAs (NMU, CRLF1, NQO1, COL3A1, TPBG, KCNK1, SLC16A3, MEST, and MAP2K6) were discovered to be shared by LUAD up-regulated genes and hypoxia up-regulated genes (Figure 2A), while seven genes (ID3, CADM1, IL18R1, LPL, EPAS1, IL6, and RGCC) were discovered to be shared by both LUAD down-regulated genes and hypoxia down (Figure 2B). These hypoxia-related genes (9 up-regulated and 7 down-regulated) and lncRNA coexpression network was constructed to identify the hypoxia-related lncRNAs. Finally, 227 hypoxia-related lncRNAs were selected ($|R^2| > 0.3$ and $P < 0.001$) (Table 2).

Identification of prognostic hypoxia-related lncRNAs signature

According to the results of univariate Cox, 20 hypoxia-related lncRNAs had a prognostic value for the patients with LUAD ($P < 0.05$, Table 3). After Lasso regression, 9 hypoxia-related lncRNAs were discovered (Figure 3, Table 4). Figure 4 showed the coexpression network and Sankey diagram of prognostic hypoxia-related lncRNAs. As shown in Figure 5, we observed a positive correlation between hypoxia-related genes and these lncRNAs. Among them, six lncRNAs (LINC00460, AL365181.2, AL606489.1, LINC02081, AC010980.2, and FAM83A-AS1) were harmful prognostic factors, and three (LINC01150, AC026355.1, and AL034397.3) were favorable prognostic factors (Figure 6, Table 5). These nine lncRNAs were utilized to establish a hypoxia-related lncRNAs signature. The formula of the risk score was as follows: risk score = (0.32223 * AC010980.2) − (0.42795 * LINC01150) + (0.138432 * AL606489.1) − (0.20391 * AL034397.3) + (0.02445 * LINC00460) + (0.16306 * LINC02081) + (0.02140 * FAM83A-AS1) + (0.05533 * AL365181.2) − (0.30018 * AC026355.1).

The prognostic influence of the established signature

The risk score was significantly associated with the overall survival (OS) of patients with LUAD. The high-risk group had shorter OS compared with the low-risk group ($P = 3.329e-09$, log-rank test) (Figure 7). Cox regression indicated significant prognostic impact of the risk score for the patients with LUAD (Figure 8).

Clinical value of the hypoxia-related lncRNAs signature

Univariate Cox regression revealed that risk score and stage

https://dx.doi.org/10.4314/mmj.v36i3.3

Table 1 Hypoxia-related genes of lung cancer in Gene Set Enrichment Analysis (GSEA) database

Type	Genes
Up-regulated	ALDH3A1 | ANP32A | BAG1 | CADM1 | CALM1 | COL15A1 | COL3A1 | CRLF1 | DMD | GSTA4 | HMOX1 | HSPA1B | ID3 | IGFBP7 | KCNK1 | LPL | MAP2K6 | MARCKS | MEST | NMU | NNMT | NQO1 | RGCC | SLC16A3 | TPBG | TPM1
Down-regulated	ALDH3A1 | ANP32A | CADM1 | CD55 | COL15A1 | COL3A1 | CRLF1 | DMD | EPAS1 | HSPA1B | ID3 | IER3 | IGFBP3 | IGFBP7 | IL18R1 | IL1A | IL6 | KCNK1 | LPL | MARCKS | MEST | MMP1 | NMU | NNMT | NRCAM | NT5E | PLA2G4A | PLAUR | RGCC | SDC4 | SLC16A3 | SOD2 | STC2 | TFPI2 | TPBG | TPM1 | UGCG | VEGFC

Table 2 The 227 hypoxia-related lncRNAs of lung adenocarcinoma (LU

AL133243.2 | AC133644.2 | LINC02100 | AC090739.1 | AC010547.2 | AC090579.1 | AP003119.1 | LINC00513 | LINC00941 | LINC02544 | LINC01150 | AP001432.1 | AC083900.1 | FP671120.4 | AC010980.2 | AC138207.4 | AP001528.2 | AC009686.2 | AC096921.2 | AC245014.3 | TMPO-AS1 | AC018653.3 | LINC01936 | AP001453.2 | AC011442.1 | AP001429.1 | LINC00467 | AC007991.2 | AL590666.2 | AL162724.1 | AP003119.2 | AL132780.1 | AC083949.1 | AC025287.3 | AC138393.3 | EP300-AS1 | AC007546.1 | AL033397.1 | AC018682.1 | MIR3945HG | AC011815.1 | AC078778.1 | AC147067.2 | TBX2-AS1 | AP005899.1 | AC005021.1 | AC004832.5 | AP002907.1 | AL606489.1 | LINC00216 | AL158166.1 | AL024508.2 | AL662844.3 | AC048341.2 | MAL2-AS1 | AC025917.1 | PITPNA-AS1 | AC131971.1 | LINC01269 | AC067817.2 |
AC130650.2 | AC104984.4 | FENDRR | AC124319.1 | AC079684.1 | TBX5-AS1 | AC027277.2 | AC091057.1 | DRAIC | AC027228.2 | AC007038.2 | LINC01607 | AC011676.1 | AC093278.2 | AL645608.8 | MIR31HG | AP001160.4 | AL365356.5 | KCNMB2-AS1 | DLEU2 | MACC1-AS1 | AC114488.1 | SAP30L-AS1 | AC006017.1 | AP000695.2 | AC026785.3 | AC010168.2 | AC020913.3 | AL034397.3 | AC005856.1 | CR936218.1 | LINC00460 | LINC01614 | AC079907.1 | LUCAT1 | AC104695.3 | AC015813.1 | AC004596.1 | AL109914.1 | AC090772.3 | AC010834.3 | HM13-IT1 | AL157838.1 | LINC01943 | AP000866.6 | AC010186.3 | AC107959.3 | AL355488.1 | AC021016.2 | LINC00942 | LINC02081 | AC245884.8 | AC093110.1 | MYO16-AS1 | AC004908.2 | MYOSLID | MBNL1-AS1 | AC022784.5 | LINC00894 | AP000692.1 | AC016590.2 | AC084117.1 | AP001189.3 | AC253576.2 | PCAT19 | AC008115.3 | AL049869.3 | AC099850.3 | AP003170.3 | AC108134.3 | AC026202.2 | AC005519.1 | LINC02122 | AL136115.2 | AC138932.5 | MAGI2-AS3 | AL031717.1 | AL162724.2 | LINC00630 | AC108727.1 | AC004253.1 | AC093788.1 | AC007014.2 | AC012073.1 | AF131215.5 | AL513327.1 | LINC00973 | AL512353.1 | AC078883.1 | MCM3AP-AS1 | AC010542.5 | AL590723.1 | AP002336.2 | AC026369.3 | AC037198.1 | ALMS1-IT1 | AC010201.2 | HIF1A-AS2 | AC004466.3 | AC008870.2 | MIR193BHG | AC127024.4 | AC022150.4 | LINC00511 | SNHG1 | LANCL1-AS1 | AC079384.1 | AC092687.3 | FAM83A-AS1 | AL365277.1 | MIR155HG | AC009275.1 | AP000786.1 | AL133355.1 | AC018755.4 | AC145207.8 | Z82243.1 | AL365181.3 | FOXP4-AS1 | AL022067.1 | AC002128.2 | AL109761.1 | P001033.2 | NEAT1 | AC063965.1 | LINP1 | NARF-IT1 | LINC01836 | AC027288.3 | AL365181.2 | AL359697.1 | AL109614.1 | AC026355.1 | AL442125.2 | AL513365.2 | AP000873.2 | MIR22HG | AC099343.2 | DLEU1 | ALG13-AS1 | AC007249.1 | AL683807.1 | SMIM25 | AC025171.3 | AC092115.3 | AL928654.1 | AL353804.2 | AC022211.1 | AL354989.1 | ANKRD10-IT1 | HSPC324 | AC002128.1 | LINC01355 | AC004884.2 | AC097641.2 | AC026356.1 | C20orf197 | AF117829.1 | AL354719.2 | AL035409.1 |
AC073316.2 | AP000695.1 | AL391427.1 | ELF3-AS1 | AL355075.2 | PRRT3-AS1 | AC008669.1

Table 3 Univariate cox results of hypoxia-related lncRNA based on TCGA-LUAD data

lncRNA	KM	B	SE	HR	HR.95L	HR.95H	p-value
LINC01150	0.0154	-0.50957	0.190111	0.600755	0.41388	0.872007	0.007354
AC010980.2	0.003607	0.282903	0.086847	1.326977	1.11928	1.573214	0.001124
AP001453.2	0.01057	0.057147	0.02399	1.058811	1.010179	1.109785	0.017214
AL606489.1	0.000851	0.182138	0.046646	1.19978	1.094954	1.31464	9.44E-05
FENDRR	0.017209	-0.36127	0.13778	0.696792	0.531894	0.912812	0.00874
AC093278.2	0.035723	-0.21798	0.109936	0.804142	0.648269	0.997493	0.047391
AP000695.2	0.00327	0.335042	0.092891	1.397999	1.1653	1.677166	0.00031
AL034397.3	0.000174	-0.29612	0.108249	0.743699	0.601527	0.919473	0.006228
AC005856.1	0.032812	-0.66277	0.280845	0.515424	0.297241	0.893757	0.01828
LINC00460	0.035424	0.022921	0.00831	1.023186	1.006656	1.039987	0.00581
LINC02081	0.006379	0.113238	0.041578	1.119898	1.032255	1.214983	0.00646
AC099850.3	0.015386	0.045118	0.011985	1.046152	1.021863	1.071018	0.000167
AF131215.5	0.005534	-0.33959	0.133239	0.712064	0.548411	0.924553	0.010812
AC026369.3	0.009687	-0.21522	0.089717	0.806364	0.676338	0.961388	0.016446
FAM83A-AS1	0.009499	0.035622	0.010357	1.036264	1.015441	1.057515	0.000583
AL365181.2	0.048168	0.061963	0.01839	1.063923	1.026259	1.10297	0.000753
AC026355.1	0.000146	-0.28476	0.08401	0.752192	0.637997	0.886826	0.0007
HSPC324	0.009531	-0.62362	0.204554	0.536002	0.358963	0.800356	0.002299
C20orf197	0.001484	-0.11343	0.054822	0.892769	0.801816	0.99404	0.038546
AP000695.1	0.007595	0.223142	0.067199	1.249998	1.095745	1.425965	0.000898

Table 4 LASSO regression coefficients of nine hypoxia-related lncRNAs

lncRNA	Coefficient	HR	HR.95L	HR.95H	p-value
LINC01150	-0.42795	0.651846	0.426544	0.996153	0.047954
AC010980.2	0.322259	1.380243	1.14761	1.660032	0.000622
AL606489.1	0.138432	1.148471	1.008348	1.308066	0.037052
AL034397.3	-0.20391	0.815536	0.670968	0.991252	0.040539
LINC00460	0.024453	1.024755	1.007387	1.042422	0.005049
LINC02081	0.163063	1.177111	1.041602	1.33025	0.008971
FAM83A-AS1	0.021398	1.021629	0.994715	1.049271	0.116194
AL365181.2	0.055328	1.056887	1.014126	1.101453	0.00865
AC026355.1	-0.30018	0.740687	0.631686	0.868496	0.000219

Table 5 Multivariate Cox results of lncRNAs based on TCGA-LUAD data

lncRNA	Coefficient	HR	HR.95L	HR.95H	p-value
LINC01150	-0.42795	0.651846	0.426544	0.996153	0.047954
AC010980.2	0.322259	1.380243	1.14761	1.660032	0.000622
AL606489.1	0.138432	1.148471	1.008348	1.308066	0.037052
AL034397.3	-0.20391	0.815536	0.670968	0.991252	0.040539
LINC00460	0.024453	1.024755	1.007387	1.042422	0.005049
LINC02081	0.163063	1.177111	1.041602	1.33025	0.008971
FAM83A-AS1	0.021398	1.021629	0.994715	1.049271	0.116194
AL365181.2	0.055328	1.056887	1.014126	1.101453	0.00865
AC026355.1	-0.30018	0.740687	0.631686	0.868496	0.000219

Table 6 Clinical characteristics and risk scores of lung adenocarcinoma using univariate cox regression

Variable	B	SE	Z	HR	HR.95L	HR.95H	p-value
Age	-0.00347	0.009599	-0.36166	0.996534	0.977961	1.015461	0.71761
Gender	1.17E-05	0.186484	6.28E-05	1.000012	0.693857	1.441253	0.99995
Stage	0.499618	0.084733	5.896378	1.648091	1.395907	1.945835	3.72E-09
T	0.470248	0.112135	4.193574	1.600391	1.284625	1.993775	2.75E-05
M	0.558732	0.306235	1.824523	1.748454	0.959372	3.186556	0.068073
N	0.580724	0.104857	5.538258	1.787332	1.455295	2.195126	3.05E-08
RiskScore	0.410106	0.049371	8.306557	1.506977	1.367986	1.660089	9.85E-17

Table 7 Clinical characteristics and risk scores of LUAD using multivariate Cox regression

Variable	B	SE	Z	HR	HR.95L	HR.95H	p-value
Age	0.000858	0.00961	0.089306	1.000859	0.982184	1.019888	0.928838
Gender	-0.15414	0.19139	-0.80536	0.857153	0.589043	1.247297	0.42061
Stage	0.498721	0.255521	1.951786	1.646615	0.997912	2.717012	0.050964
T	0.0711	0.127703	0.556762	1.073689	0.835945	1.379047	0.57769
M	-0.59991	0.674064	-0.88999	0.548862	0.146453	2.056967	0.373473
N	0.079815	0.220549	0.361892	1.083087	0.702961	1.668764	0.717432
RiskScore	0.360784	0.052757	6.838604	1.434454	1.29354	1.590719	8.00E-12

Table 8 Clinical influences of risk score signature for TCGA-LUAD data

Clinical	Group	n	Mean	SD	t	P
Age	> 65	168	1.635	1.984	0.729059	0.467
	≤ 65	157	1.493	1.493		
Gender	Femal	164	1.523	1.547	-0.4459	0.656
	Male	161	1.611	1.962		
Stage	I-II	245	1.283	1.113	-3.56944	0.001
	III-IV	80	2.434	2.812		
T	T1-2	281	1.38	1.193	-2.56003	0.014
	T3-4	44	2.755	3.531		
M	M0	304	1.506	1.661	-1.53458	0.140
	M1	21	2.444	2.768		
N	N0	205	1.349	1.654	-2.84986	0.005
	N1-3	120	1.939	1.883		

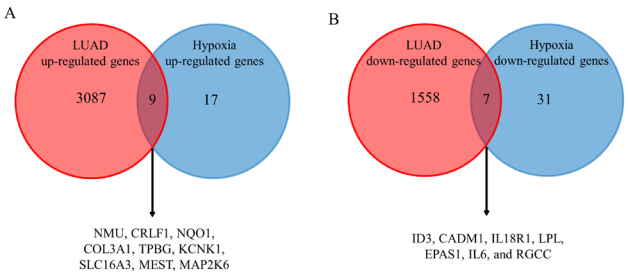

Figure 2 Number of intersecting genes between the (A) up-regulated and (B) down-regulated different expression genes (DEGs) of lung adenocarcinoma and hypoxia-related genes

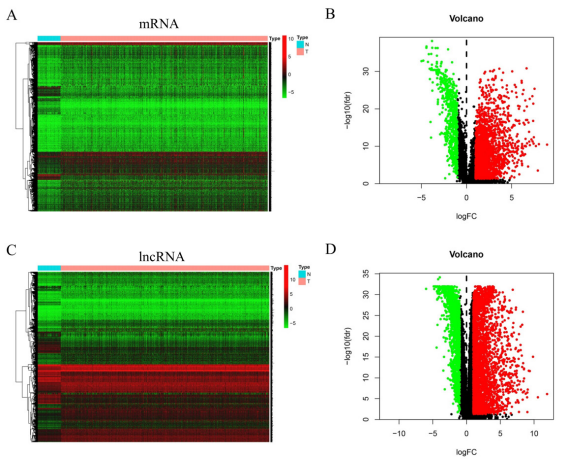

Figure 1 Identification of differentially expressed genes (DEGs) in lung adenocarcinoma (LUAD) from TCGA datasets. (A) The heatmap and (B) volcano plot of DEGs of mRNA in LUAD. (C) The heatmap and (D) volcano plot of DEGs of long noncoding RNAs (lncRNAs) in LUAD. T: tumor; N: control

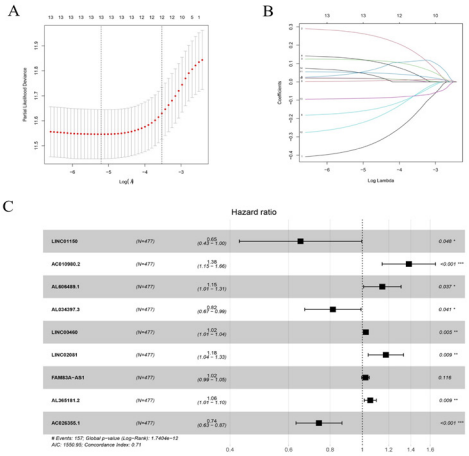

Figure 3 Hypoxia-related lncRNAs selection utilizing Lasso model. (A) Lasso coefficient values of 9 hypoxia-related lncRNAs in lung adenocarcinoma (LUAD). The vertical dashed lines are at the optimal log (lambda) value. (B) Profiles of Lasso coefficients. (C) Forest plot for 9 hypoxia-related lncRNAs in LUAD.

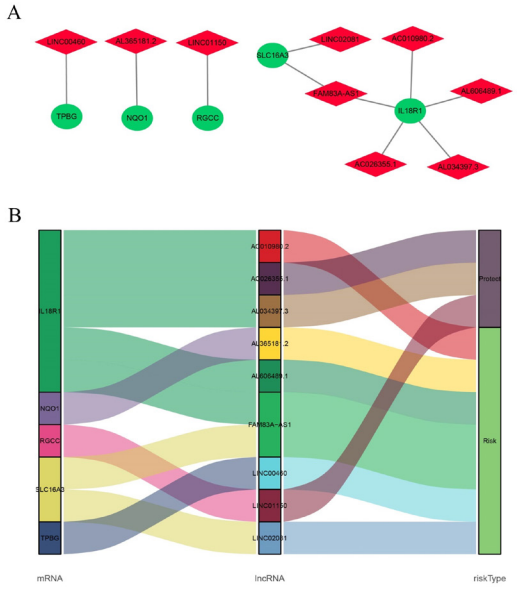

Figure 4 The coexpression network and Sankey diagram of prognostic hypoxia-related lncRNAs. (A) The coexpression network between prognostic lncRNAs and hypoxia-related genes in lung adenocarcinoma. Red diamond nodes represent prognostic lncRNAs, and the sky blue round nodes represent hypoxia-related genes. The coexpression network was visualized using Cytoscape 3.6.1 software. (B) Sankey diagram showed the association between prognostic hypoxia-related lncRNAs, hypoxia-related genes, and risk types

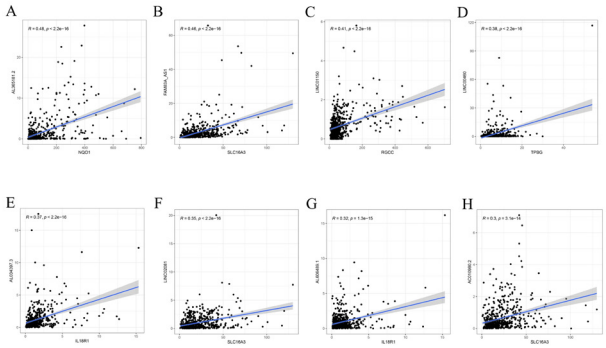

Figure 5 Correlation between hypoxia-related lncRNAs and hypoxia-related genes. (A) AL365181.2 and NQO1. (B) FAM83A-AS1 and SLC16A3. (C) LINC01150 and RGCC. (D) LINC00460 and TPBG. (E) AL034397.3 and IL18R1. (F) LINC02081 and SLC16A3. (G) AL606489.1 and IL18R1. (G) AL606489.1 and IL18R1. (F) AC010980.2 and SLC16A3

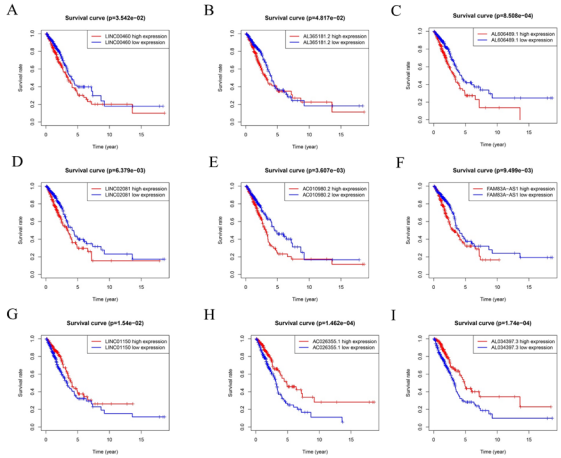

Figure 6 The KM survival curves of nine prognostic hypoxia-related lncRNAs. Six hypoxia-related lncRNAs (LINC00460, AL365181.2, AL606489.1, LINC02081, AC010980.2, and FAM83A-AS1) were independent unfavorable factors. Three lncRNAs (LINC01150, AC026355.1, and AL034397.3) were independent beneficial factors for lung adenocarcinoma

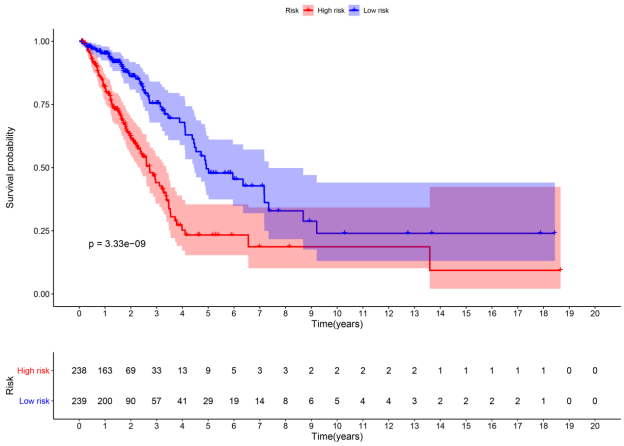

Figure 7 The KM survival curve of risk score based on nine hypoxia-related lncRNAs

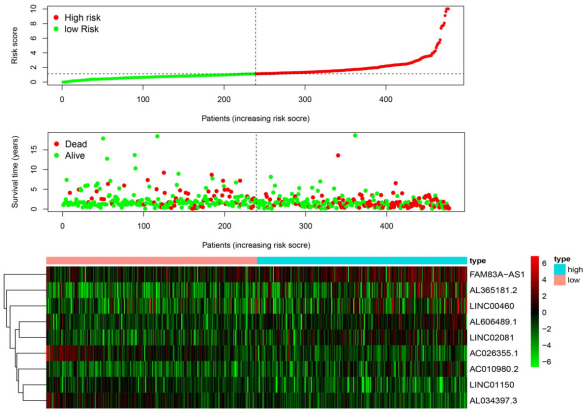

Figure 8 The analysis of hypoxia-related lncRNA signature for patients with lung adenocarcinoma. (A) The risk score between the high-risk group and the low-risk group. (B) The survival time of the patients. (C) Heat map of nine hypoxia-related lncRNAs' expression. The color from green to red reveals a rising tendency from low to high levels

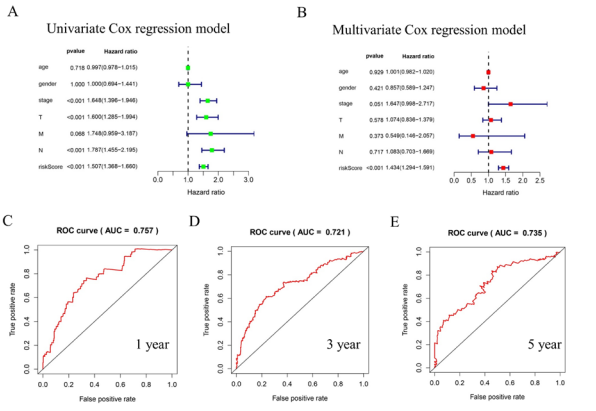

Figure 9 Prognostic indicators based on hypoxia-related lncRNAs showed great predictive performance. The forest plots for univariate (A) and multivariate (B) Cox regression analysis in lung adenocarcinoma. The areas under the ROC curve about (C) 1 year, (D) 3 years, and (E) 5 years

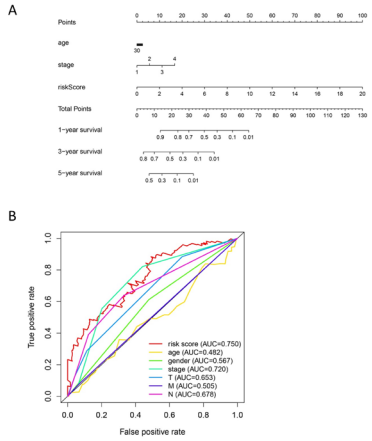

Figure 10 The evaluation of prognostic models based on nine hypoxia-related lncRNAs. (A) The nomogram of 1-year, 3-year or 5-year OS based on risk score, age, and TNM stage. (B) The ROC curves analysis based on risk score and the clinicopathologic parameters

were independent prognostic indicators, and HR of risk score was 1.507 (95% CI: 1.368–1.660, P < 0.001, Table 6, Figure 9A). After controlling clinical features, risk score remained an independent prognostic indicator in multivariate analysis (HR = 1.434, 95% CI = 1.294 − 1.591, P < 0.001, Table 7, Figure 9B). The areas under the ROC curve corresponding to 1 year, 3 years, and 5 years of survival were 0.757, 0.721, and 0.735, respectively (Figure 9C, 9D and 9E). Risk score, age, and TNM stage were included in the nomogram. As indicated in the nomogram, risk score and TNM stage were the largest contribution to 1-, 3- and 5-year OS of patients with lung adenocarcinoma (Figure 10A). The C-index of the prognostic model was 0.759 (95% CI: 0.710-0.808). The AUC of five-year survival rate showed that risk score (0.750) and stage (0.720) had a certain prediction ability (Figure 10B). The risk scores increased with stage, demonstrating that this hypoxia-related lncRNAs signature may be related to the progression of lung adenocarcinoma (Table 8).

Discussion

Dysregulation of hypoxia has been associated with a number of diseases, including cancer, myocardial infarction, chronic obstructive pulmonary disease, obesity, Coronavirus Disease 2019 (COVID-19), and others[20,25-27]. lncRNAs played an indispensable role in different aspects of tumorigenesis which were considered a new type of biomarkers in cancer diagnosis, prognosis and therapeutic[28,29]. However, most researches focused on the function of specific genes involved in hypoxia[30,31]. There are no systematic studies about hypoxia-related lncRNAs signatures to predict the survival of patients with LUAD. Therefore, it was necessary to establish a hypoxia-related lncRNAs signature to predict the prognosis of patients with LUAD based on the large-scale databases.

In the present study, lncRNAs were screened for hypoxia-relatedness by constructing a coexpression network of lncRNA and genes important for hypoxia. Lasso regression and Cox regression were also used to identify the nine predictive hypoxia-related lncRNAs: LINC00460, AL365181.2, AL606489.1, LINC02081, AC010980.2, FAM83A-AS1, LINC01150, AC026355.1, and AL034397.3. The nine hypoxia-related lncRNAs may act as prognostic molecular markers of prognosis and therapeutic targets for LUAD patients. According to our knowledge, this is the first study to identify a signature of hypoxia-related lncRNAs that can be used to predict the prognosis of LUAD patients utilizing huge databases.

Four hypoxia-related lncRNAs (LINC00460, FAM83A-AS1, AC026355.1, and AL034397.3) were reported to be associated with LUAD[32-35]. For example, LINC00460 promotes tumor growth of human lung adenocarcinoma by targeting miR-302c-5p/FOXA1 axis[34]. LINC00460 can also promote cell migration and invasion through regulating epithelial-mesenchymal transition (EMT) in non-small cell lung cancer[35,36]. A recent study shows that LINC00460 plays a pivotal role in gefitinib resistance of NSCLC cells by targeting EGFR through sponging miR-769-5p[37]. Wang et al. revealed that FAM83A-AS1 increased FAM83A expression by enhancing FAM83A pre-mRNA stability and promoted the tumorigenesis of LUAD, revealing that FAM83A-AS1 was a risk factor and possessed oncogenic functions in LUAD[38]. It was found that FAM83A-AS1 enhances cell migration, invasion and EMT by modulating the miR-150-5p/MMP14 pathway in LUAD33. For the five remaining hypoxia-related lncRNAs (AL365181.2, AL606489.1, LINC02081, AC010980.2, and LINC01150), there were no studies to report their prognostic roles in cancer, as well as LUAD. Thus, more researches were necessary to explore how these lncRNAs affect the prognosis of patients with LUAD through hypoxia exactly.

The prognosis of LUAD patients was significantly predicted by a signature made up of 9 hypoxia-related lncRNAs. The areas under the ROC curve corresponding to 1 year, 3 years, and 5 years of survival were 0.757, 0.721, and 0.735, respectively. This outcome suggested that the risk score signature had some potential in survival prediction. The signature might be employed as an independent prognostic factor, according to both univariate and multivariate Cox analyses. The C-index, ROC curve, and calibration curve findings showed that the model had superior discrimination and accuracy, suggesting that it might be used as a possible prognostic tool for LUAD patients. These findings are helpful in our investigation of how hypoxia-related lncRNAs function. There were several restrictions on the current investigation. Firstly, the data source of this study is single, and the amount of data included is not large, so the analysis results may have certain deviation. Secondly, our study is a retrospective study, and more prospective studies will be required to prove the prognostic function of hypoxia-related signals. Thirdly, in order to ensure the robustness of the prognostic model, the prognostic model of our established model is required to be further confirmed in other independent cohorts to ensure its robustness. Finally, the functional experiments should be conducted to further indicate the potential molecular mechanisms for predicting the effect of hypoxia-related lncRNAs.

Conclusion

The hypoxia-related lncRNAs signature which was composed of nine hypoxia-related lncRNAs was used to differentiate patients at different risks, and it was a significantly independent factor for the patients with LUAD. Therefore, the nine hypoxia-related lncRNAs and their signature might be molecular biomarkers and therapeutic targets for the patients with LUAD.

Acknowledgements

This work was supported by the Natural Science Foundation

of Shaanxi Province (Grant No. 2024JC-YBQN-0927 and No. 2023-JC-QN-0979), the Key Research and Development Programs of Shaanxi Province (Grant No. 2021SF-322), and the Integration of Basic and Clinical Science Project of School of Basic Medical Sciences, Xi'an Jiaotong University (Grant No. YXJLRH2022034).

Conflicts of interest

The authors declare that they have no known competing financial interests or personal relationships that could have appeared to influence the work reported in this paper.

Data availability statement

The datasets used and analyzed during the current study are available from the corresponding author on reasonable request.

References

1. Bade BC, Dela Cruz CS. Lung Cancer 2020: Epidemiology, Etiology, and Prevention. Clin Chest Med. 2020 Mar;41(1):1-24. doi: 10.1016/j.ccm.2019.10.001.

2. Nasim F, Sabath BF, Eapen GA. Lung Cancer. Med Clin North Am. 2019 May;103(3):463-473. doi: 10.1016/j.mcna.2018.12.006.

3. Cao M, Chen W. Epidemiology of lung cancer in China. Thorac Cancer. 2019 Jan;10(1):3-7. doi: 10.1111/1759-7714.12916.

4. Lemjabbar-Alaoui H, Hassan OU, Yang YW, Buchanan P. Lung cancer: Biology and treatment options. Biochim Biophys Acta. 2015 Dec;1856(2):189-210. doi: 10.1016/j.bbcan.2015.08.002.

5. Nawaz K, Webster RM. The non-small-cell lung cancer drug market. Nat Rev Drug Discov. 2016 Apr;15(4):229-30. doi: 10.1038/nrd.2016.42.

6. Pao W, Girard N. New driver mutations in non-small-cell lung cancer. Lancet Oncol. 2011 Feb;12(2):175-80. doi: 10.1016/S1470-2045(10)70087-5.

7. He D, Wang D, Lu P, Yang N, Xue Z, Zhu X et al. Single-cell RNA sequencing reveals heterogeneous tumor and immune cell populations in early-stage lung adenocarcinomas harboring EGFR mutations. Oncogene. 2021 Jan;40(2):355-368. doi: 10.1038/s41388-020-01528-0.

8. Martins-Filho SN, Weiss J, Pham NA, Li Q, Cabanero M, Fares A et al. EGFR-mutated lung adenocarcinomas from patients who progressed on EGFR-inhibitors show high engraftment rates in xenograft models. Lung Cancer. 2020 Jul;145:144-151. doi: 10.1016/j.lungcan.2020.03.022.

9. Xu JY, Zhang C, Wang X, Zhai L, Ma Y, Mao Y et al. Integrative Proteomic Characterization of Human Lung Adenocarcinoma. Cell. 2020 Jul 9;182(1):245-261.e17. doi: 10.1016/j.cell.2020.05.043.

10. Wilson WR, Hay MP. Targeting hypoxia in cancer therapy. Nat Rev Cancer. 2011 Jun;11(6):393-410. doi: 10.1038/nrc3064.

11. Mao X, Nanzhang, Xiao J, Wu H, Ding K. Hypoxia-Induced Autophagy Enhances Cisplatin Resistance in Human Bladder Cancer Cells by Targeting Hypoxia-Inducible Factor-1α. J Immunol Res. 2021 Feb 17;2021:8887437. doi: 10.1155/2021/8887437.

12. Sheng Y, Li J, Yang Y, Lu Y. Hypoxia-inducible lipid droplet-associated (HILPDA) facilitates the malignant phenotype of lung adenocarcinoma cells in vitro through modulating cell cycle pathways. Tissue Cell. 2021 Jun;70:101495. doi: 10.1016/j.tice.2021.101495.

13. Sun J, Xiong Y, Jiang K, Xin B, Jiang T, Wei R et al. Hypoxia-sensitive long noncoding RNA CASC15 promotes lung tumorigenesis by regulating the SOX4/β-catenin axis. J Exp Clin Cancer Res. 2021 Jan 6;40(1):12. doi: 10.1186/s13046-020-01806-5.

14. Tian T, Dong Y, Zhu Y, Chen Y, Li X, Kuang Q et al. Hypoxia-induced CNPY2 upregulation promotes glycolysis in cervical cancer through activation of AKT pathway. Biochem Biophys Res Commun. 2021 Apr 30;551:63-70. doi: 10.1016/j.bbrc.2021.02.116.

15. Mercer TR, Dinger ME, Mattick JS. Long non-coding RNAs: insights into functions. Nat Rev Genet. 2009 Mar;10(3):155-9. doi: 10.1038/nrg2521.

16. White NM, Cabanski CR, Silva-Fisher JM, Dang HX, Govindan R, Maher CA. Transcriptome sequencing reveals altered long intergenic non-coding RNAs in lung cancer. Genome Biol. 2014 Aug 13;15(8):429. doi: 10.1186/s13059-014-0429-8.

17. Xu G, Chen J, Pan Q, Huang K, Pan J, Zhang W et al. Long noncoding RNA expression profiles of lung adenocarcinoma ascertained by microarray analysis. PLoS One. 2014 Aug 4;9(8):e104044. doi: 10.1371/journal.pone.0104044.

18. Xu XL, Gong Y, Zhao DP. Elevated PHD2 expression might serve as a valuable biomarker of poor prognosis in lung adenocarcinoma, but no lung squamous cell carcinoma. Eur Rev Med Pharmacol Sci. 2018 Dec;22(24):8731-8739. doi: 10.26355/eurrev_201812_16638.

19. Zhou W, Zhang S, Li HB, Cai Z, Tang S, Chen LX et al. Development of Prognostic Indicator Based on Autophagy-Related lncRNA Analysis in Colon Adenocarcinoma. Biomed Res Int. 2020 Sep 2;2020:9807918. doi: 10.1155/2020/9807918.

20. Terker AS, Sasaki K, Arroyo JP, Niu A, Wang S, Fan X et al. Activation of hypoxia-sensing pathways promotes renal ischemic preconditioning following myocardial infarction. Am J Physiol Renal Physiol. 2021 Apr 1;320(4):F569-F577. doi: 10.1152/ajprenal.00476.2020.

21. Wu F, Zhao Z, Chai RC, Liu YQ, Li GZ, Jiang HY et al. Prognostic power of a lipid metabolism gene panel for diffuse gliomas. J Cell Mol Med. 2019 Nov;23(11):7741-7748. doi: 10.1111/jcmm.14647.

22. Xing XL, Yao ZY, Zhang T, Zhu N, Liu YW, Peng J. MicroRNA-Related Prognosis Biomarkers from High-Throughput Sequencing Data of Colorectal Cancer. Biomed Res Int. 2020 Sep 9;2020:7905380. doi: 10.1155/2020/7905380.

23. Zhuo S, Chen Z, Yang Y, Zhang J, Tang J, Yang K. Clinical and Biological Significances of a Ferroptosis-Related Gene Signature in Glioma. Front Oncol. 2020 Nov 20;10:590861. doi: 10.3389/fonc.2020.590861.

24. Zhang M, Wang X, Chen X, Zhang Q, Hong J. Novel Immune-Related Gene Signature for Risk Stratification and Prognosis of Survival in Lower-Grade Glioma. Front Genet. 2020 Apr 15;11:363. doi: 10.3389/fgene.2020.00363.

25. AbdelMassih A, Yacoub E, Husseiny RJ, Kamel A, Hozaien R, El Shershaby M et al. Hypoxia-inducible factor (HIF): The link between obesity and COVID-19. Obes Med. 2021 Mar;22:100317. doi: 10.1016/j.obmed.2020.100317.

26. Vinaiphat A, Low JK, Yeoh KW, Chng WJ, Sze SK. Application of Advanced Mass Spectrometry-Based Proteomics to Study Hypoxia Driven Cancer Progression. Front Oncol. 2021 Feb 23;11:559822. doi: 10.3389/fonc.2021.559822.

27. Wu G, Lee YY, Gulla EM, Potter A, Kitzmiller J, Ruben MD et al. Short-term exposure to intermittent hypoxia leads to changes in gene expression seen in chronic pulmonary disease. Elife. 2021 Feb 18;10:e63003. doi: 10.7554/eLife.63003.

28. Chen Y, Feng W, Ye K, Guo L, Xia H, Guan Y et al. Application of Metagenomic Next-Generation Sequencing in the Diagnosis of Pulmonary Infectious Pathogens From Bronchoalveolar Lavage Samples. Front Cell Infect Microbiol. 2021 Mar 11;11:541092. doi: 10.3389/fcimb.2021.541092.

29. Goyal B, Yadav SRM, Awasthee N, Gupta S, Kunnumakkara AB, Gupta SC. Diagnostic, prognostic, and therapeutic significance of long non-coding RNA MALAT1 in cancer. Biochim Biophys Acta Rev Cancer. 2021 Apr;1875(2):188502. doi: 10.1016/j.bbcan.2021.188502.

30. Li X, Li Y, Bai S, Zhang J, Liu Z, Yang J. NR2F1-AS1/miR-140/HK2 Axis Regulates Hypoxia-Induced Glycolysis and Migration in Hepatocellular Carcinoma. Cancer Manag Res. 2021 Jan 15;13:427-437. doi: 10.2147/CMAR.S266797.

31. Wang J, Zhai C, Wang Q, Shi W, Fang W, Yan X et al. Determinants of ICS therapy adherence in patients with asthma. Am J Manag Care. 2021 Feb 1;27(2):e36-e41. doi: 10.37765/ajmc.2021.88587.

32. Chai L, Feng W, Zhai C, Shi W, Wang J, Yan X et al. The association between cystatin C and COPD: a meta-analysis and systematic review. BMC Pulm Med. 2020 Jun 26;20(1):182. doi: 10.1186/s12890-020-01208-5.

33. Xiao G, Wang P, Zheng X, Liu D, Sun X. FAM83A-AS1 promotes lung adenocarcinoma cell migration and invasion by targeting miR-150-5p and modifying MMP14. Cell Cycle. 2019 Nov;18(21):2972-2985. doi: 10.1080/15384101.2019.1664225.

34. Ye JJ, Cheng YL, Deng JJ, Tao WP, Wu L. LncRNA LINC00460 promotes tumor growth of human lung adenocarcinoma by targeting miR-302c-5p/FOXA1 axis. Gene. 2019 Feb 15;685:76-84. doi: 10.1016/j.gene.2018.10.058.

35. Yue QY, Zhang Y. Effects of Linc00460 on cell migration and invasion through regulating epithelial-mesenchymal transition (EMT) in non-small cell lung cancer. Eur Rev Med Pharmacol Sci. 2018 Feb;22(4):1003-1010. doi: 10.26355/eurrev_201802_14382.

36. Li K, Sun D, Gou Q, Ke X, Gong Y, Zuo Y et al. Long non-coding RNA linc00460 promotes epithelial-mesenchymal transition and cell migration in lung cancer cells. Cancer Lett. 2018 Apr 28;420:80-90. doi: 10.1016/j.canlet.2018.01.060.

37. Ma G, Zhu J, Liu F, Yang Y. Long Noncoding RNA LINC00460 Promotes the Gefitinib Resistance of Nonsmall Cell Lung Cancer Through Epidermal Growth Factor Receptor by Sponging miR-769-5p. DNA Cell Biol. 2019 Feb;38(2):176-183. doi: 10.1089/dna.2018.4462.

38. Wang W, Zhao Z, Xu C, Li C, Ding C, Chen J et al. LncRNA FAM83A-AS1 promotes lung adenocarcinoma progression by enhancing the pre-mRNA stability of FAM83A. Thorac Cancer. 2021 May;12(10):1495-1502. doi: 10.1111/1759-7714.13928.